REVIEW ARTICLE

Pulse Inversion Techniques in Ultrasonic Nonlinear Imaging

Che-Chou Shen, Yi-Hong Chou[1,2], Pai-Chi Li[3]*

Pulse inversion (PI) technique plays an important role in ultrasonic nonlinear imaging. For tissue imaging, PI technique provides suppression of spectral leakage and, thus, produces better image contrast. For contrast imaging, contrast between the agents and surrounding tissues are also enhanced with this technique by distinguishing nonlinear microbubbles from the background in either Doppler domain or radiofrequency domain. This paper reviews the theoretical backgrounds and relevant issues of the PI technique. Improvements in image contrast with the PI technique in both tissue harmonic imaging and contrast harmonic imaging are discussed in detail. In addition, potential motion artifacts and related contrast degradation are also included.

KEY WORDS — contrast detection, motion artifacts, nonlinear imaging, pulse inversion, ultrasonic contrast agents

■ *J Med Ultrasound* 2005;13(1):3–17 ■

Introduction

Ultrasonic nonlinear imaging has demonstrated that it can provide superior image quality compared to conventional linear imaging, and it has become an important diagnostic tool in many clinical applications [1–5]. Nonlinear imaging differs from linear imaging in the mechanism of signal generation. In linear imaging, echoes linearly backscattered in the fundamental frequency band are used for imaging. In nonlinear imaging, however, generation of nonlinear echoes depends on the nonlinear properties of the imaged target and the propagation medium. In clinical applications, two sources contribute to nonlinear echoes: human tissues and ultrasound contrast agents (UCAs), which are usually introduced into the vascular beds via intravenous administration.

Nonlinear tissue signals are generated when the acoustic wave propagates in human tissues. Note that the acoustic velocity increases with the instantaneous pressure and the nonlinear characteristic of propagation tissue [6–10]. As a result of pressure-dependent velocity, the high-pressure crest propagates faster than the low-pressure trough when the original transmit signal is propagating in a nonlinear tissue. Over a distance of propagation, this leads to the progressive steepening of the ultrasound waveform. This process is referred to as *finite amplitude distortion*, which is characterized by the

Department of Electrical Engineering, National Taiwan University of Science and Technology, [1]Department of Radiology, Veterans General Hospital-Taipei, [2]National Yang-Ming University School of Medicine, and [3]Department of Electrical Engineering, National Taiwan University, Taipei, Taiwan, R.O.C.

**Address correspondence to:* Dr. Che-Chou Shen, Department of Electrical Engineering, National Taiwan University of Science and Technology, 43, Section 4, Keelung Road, Taipei 106, Taiwan, R.O.C. *E-mail: choushen@mail.ntust.edu.tw*

generation of harmonic signals whose frequencies are at multiples of the original transmit frequency. The acoustic waveforms before and after the distortion are demonstrated in Fig. 1A and Fig. 1B, respectively. The corresponding spectra are shown in Fig. 2. Since the tissue harmonic signal is generated gradually throughout the propagation path, the harmonic signal is usually weak in the near field. Though the weak intensity causes difficulties in imaging the superficial structures, the reverberations from the near-field anatomy are reduced in tissue harmonic imaging.

For UCAs, the mechanism of nonlinear signal generation is completely different. UCAs are mostly comprised of microbubbles encapsulated by protective shells. To improve the stability of microbubble contrast agents, gases with high molecular weights, such as sulfur hexafluoride and perfluoropropane, are usually used as the gas core. When UCAs are injected into the blood pool, the microbubbles produce strong backscattered signals due to the acoustic-impedance mismatch between blood and air [11,12]. Therefore, UCAs are capable of enhancing both grayscale images and Doppler signals.

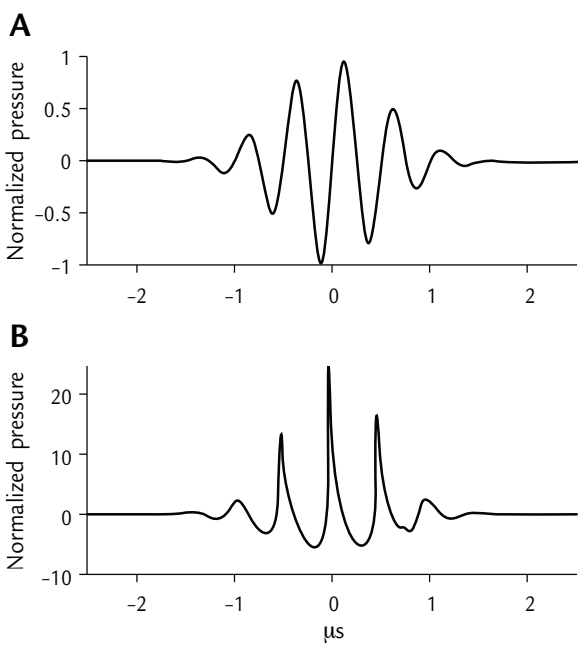

Fig. 1. *Simulated acoustic waveforms. (A) Waveform at the transducer's surface (i.e. before finite amplitude distortion). (B) Waveform at the focal point (i.e. after finite amplitude distortion).*

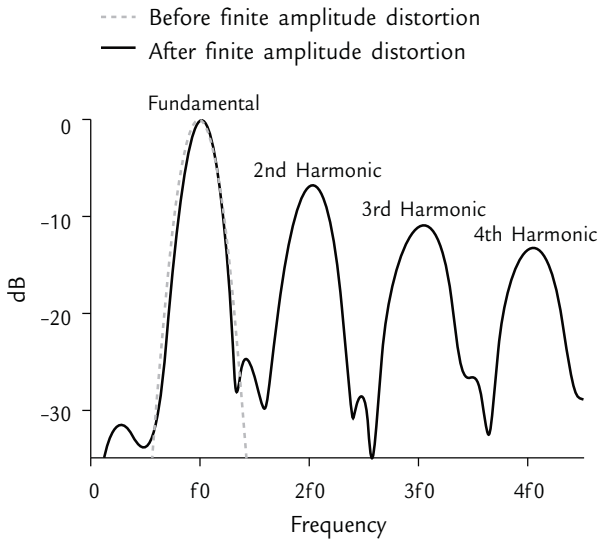

Fig. 2. *Simulated spectra of the waveforms before and after finite amplitude distortion. The dashed line represents the spectrum of the waveform in Fig. 1A and the solid line represents the spectrum of the waveform in Fig. 1B.*

One example of Doppler enhancement is demonstrated in Fig. 3. In addition, the microbubbles exhibit significant nonlinear oscillations when the impinging sound wave is near the resonance frequency of the bubbles [13]. Nonlinear responses from UCAs include harmonic and subharmonic generations [14,15]. An example of contrast harmonic imaging to evaluate a focal hepatic lesion is illustrated in Fig. 4. UCAs can be altered by exposure to intense insonification. The changes include reshaping, resizing and destruction of the bubbles [16]. UCAs may also be displaced by the acoustic radiation force [17]. Clinically, UCAs can be utilized to enhance the contrast between normal and diseased tissues, and may help to outline vessels and cardiac chambers. It can be seen in Fig. 5 that the border between the cardiac chamber and the myocardium is much better defined when intravenous administration of UCAs is applied.

Though the image contrast in nonlinear imaging is improved compared to its linear counterpart by using the nonlinear properties of either the native tissue or UCAs, the performance of nonlinear imaging is still limited. For example, the nonlinearity of the imaging system itself may degrade the image contrast [18]. It has also been shown that the

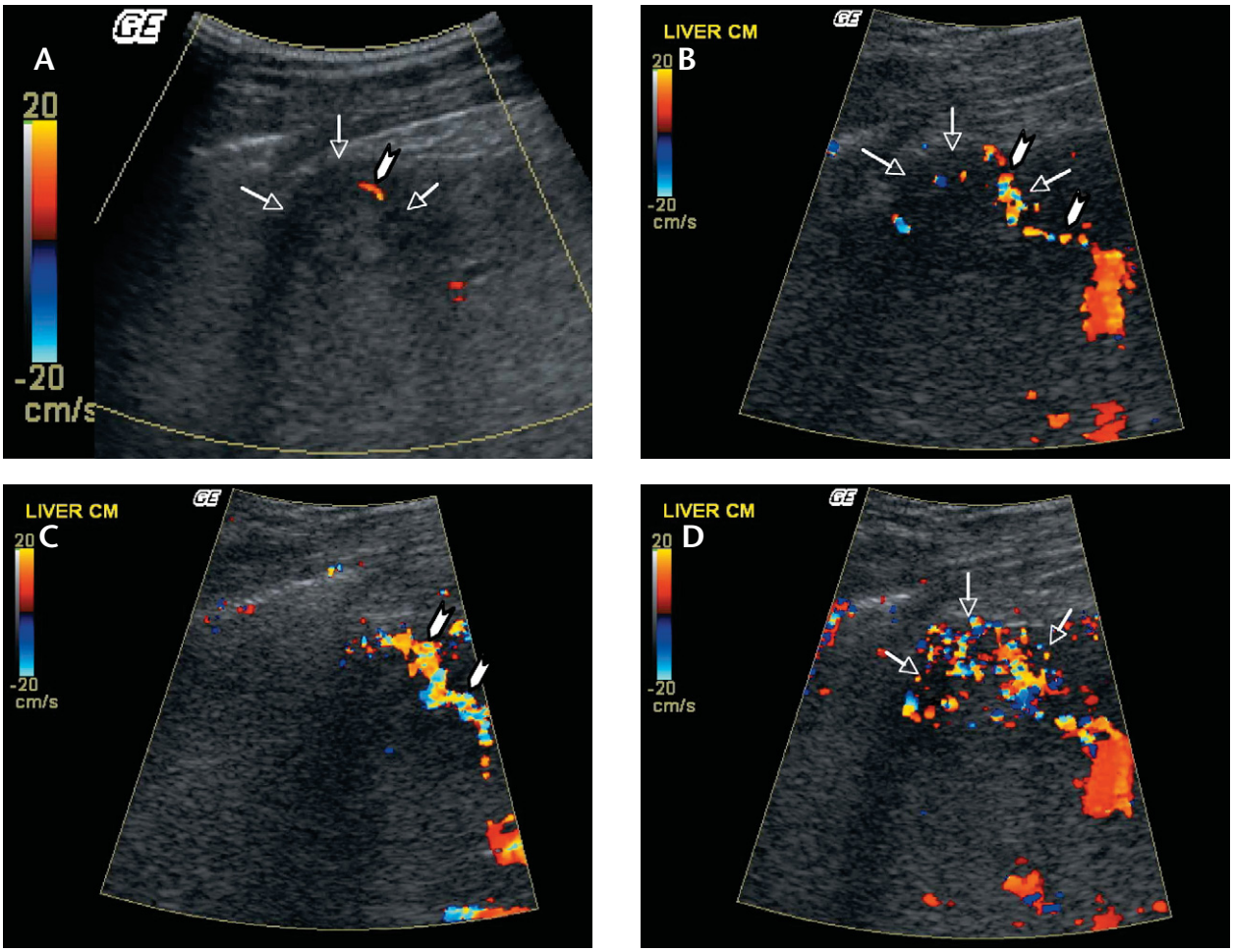

Fig. 3. *Application of microbubble ultrasonic contrast agent (Levovist®) in the color Doppler ultrasound evaluation of a small hepatic tumor (1.4 cm) (arrows). (A) Conventional color Doppler ultrasound (CDU) demonstrates only minimal color flow signals (arrowhead) in the peripheral region of the nodule. (B) CDU study 16 seconds after intravenous injection of contrast agent: a supplying artery is clearly delineated (arrowheads) to reach the tumor margin. (C) CDU study 22 seconds after contrast administration. (D) CDU study 34 seconds after contrast administration: pronounced color flow signals in the tumor are demonstrated, indicating a hypervascular tumor, confirmed histologically to be hepatocellular carcinoma.*

signal-to-noise ratio in tissue harmonic imaging is sometimes insufficient, especially in the near-field [19]. The pulse inversion (PI) technique is one of the most promising methods for improving the performance of nonlinear imaging. This paper summarizes theoretical backgrounds of the PI technique and reviews relevant issues in PI-based ultrasonic nonlinear imaging. Introductions to the PI technique in the radiofrequency (RF) domain and Doppler domain are first provided. Applications of the PI technique in both tissue harmonic imaging and contrast imaging are also introduced, and the efficacy on contrast improvement is demonstrated. In addition, potential contrast degradation resulting from the main limitation of the PI technique, motion artifacts, are also discussed.

Pulse Inversion Technique

In nonlinear imaging, the PI technique provides improved image quality and enhanced diagnostic capabilities by reducing potential interference from the linearly propagated acoustic signal. Note that the nonlinear signals from either tissue or UCAs usually appear at the harmonic bands (i.e. multi-

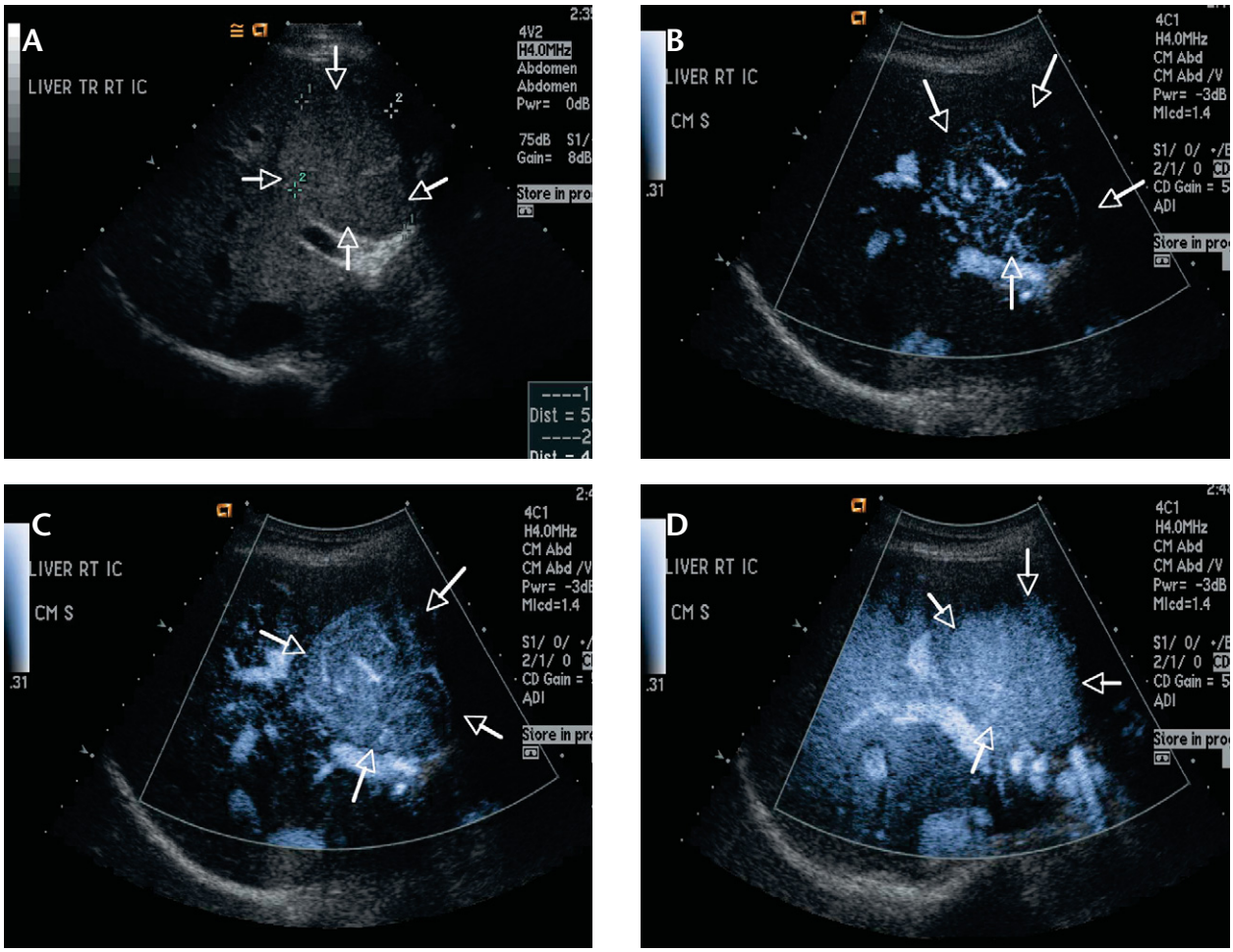

Fig. 4. *Contrast-enhanced harmonic ultrasonography using the pulse inversion technique in the evaluation of a focal hepatic lesion. (A) Grayscale ultrasonography demonstrates a focal hyperechoic lesion in the right lobe of the liver (arrows). (B) Early arterial phase (18 seconds after contrast administration) depicts tumor vessels in the lesion (arrows). (C) Late arterial phase (35 seconds after contrast administration) shows both intralesional tumor vessels and tumor stain (arrows). (D) Parenchymal phase (45 seconds after contrast administration) shows that the lesion is homogeneously enhanced (arrows), similar to the liver parenchyma. The lesion was confirmed histologically to be focal nodular hyperplasia.*

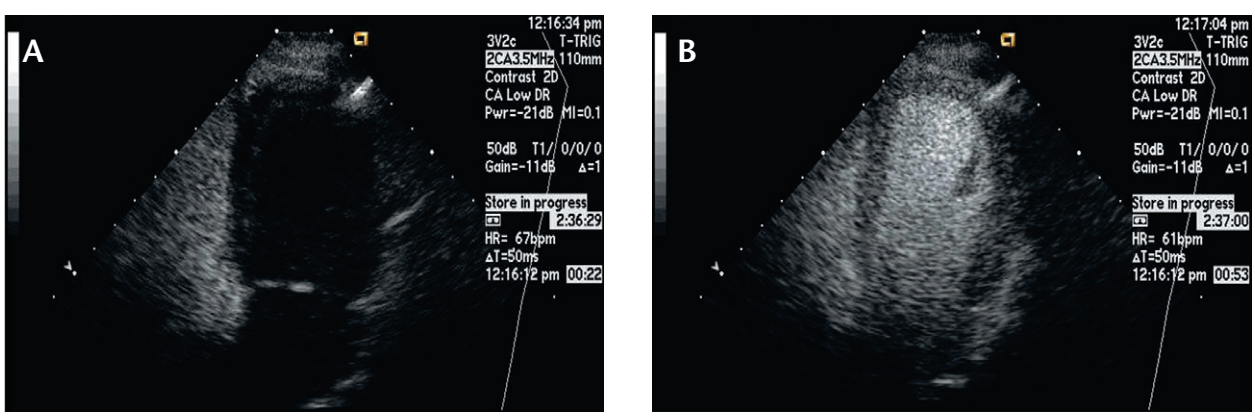

Fig. 5. *Ultrasound images of the left cardiac chambers (from www.acuson.com). (A) Before contrast agent entered the left cardiac chambers. (B) After contrast agent entered the left cardiac chambers: the arterial and ventricular lumens are well enhanced and the border of the ventricular myocardium is very well delineated.*

ples of the transmit frequency). Thus, they are often referred to as harmonic signals. Conventionally, harmonic signals are extracted from the received echo by filtering [20–22]. Although filtering can be efficiently implemented, it suffers from potential contrast degradation resulting from spectral leakage. In other words, non-negligible harmonic components may have been present at the surface of the transducer prior to propagation if the transmit bandwidth is large or the ultrasound system itself is nonlinear. Such a leakage signal propagates linearly and interferes with the nonlinearly-generated harmonic signal. The leakage signal cannot be filtered out from its nonlinear counterpart because of the spectral overlap of the two signals.

Instead of conventional filtering, the PI technique is an alternative method to extract the harmonic signals. Based on how the received echoes are processed, the PI technique can be divided into two categories: the PI technique that applies to the Doppler frequency domain and the PI technique that extracts nonlinear signals in the RF domain. In this paper, the former will be referred to as *PI Doppler* and the latter will be referred to as *RF pulse inversion*.

PI Doppler

In conventional Doppler, multiple pulses are transmitted along the same beam at a fixed pulse repetition frequency (PRF), and the pulse-to-pulse changes in the received echoes are used to estimate the movement of the imaged target. Echoes from fast moving objects (such as blood cells) will have higher Doppler frequencies, and echoes from slow moving or static objects (such as tissue around vessels) will have lower Doppler frequencies. Thus, high-pass filtering can be performed in the Doppler frequency domain to filter out Doppler signals from slow moving or static objects. This filter is usually referred to as a *clutter filter* or *wall filter*. However, the efficacy of the clutter filter is limited, especially if the surrounding tissues move at a similar velocity to blood flow. One example is the case of microperfusion, where the flow signal in the capillary and the surrounding tissue signal overlap in Doppler frequencies. As a result of the spectral overlap, the flowing blood and the tissue cannot be separated by any filtering. PI Doppler has, therefore, been proposed to overcome this problem [23,24]. In PI Doppler, the pulse sequence is similar to that in conventional Doppler, except that every second transmit pulse is inverted. In other words, a pulse-to-pulse 180° modulation of the linear echo is applied. Consequently, a PRF/2 Doppler shift is added into the linear echo while the even-order harmonics are not affected. Hence, the second harmonic signal can be effectively separated from the linear signal in Doppler frequencies when PI Doppler is applied. Doppler spectra of the linear signal and the second harmonic signal are illustrated in Fig. 6. It is assumed that a static target, which produces both the linear and the second harmonic echoes, is being detected. In other words, there is no Doppler shift in this case. In the upper panel, a conventional Doppler technique is used. Note that the spectra of the linear signal and the second harmonic signal significantly overlap at low Doppler frequencies (center at zero frequency). When PI Doppler is adopted, the

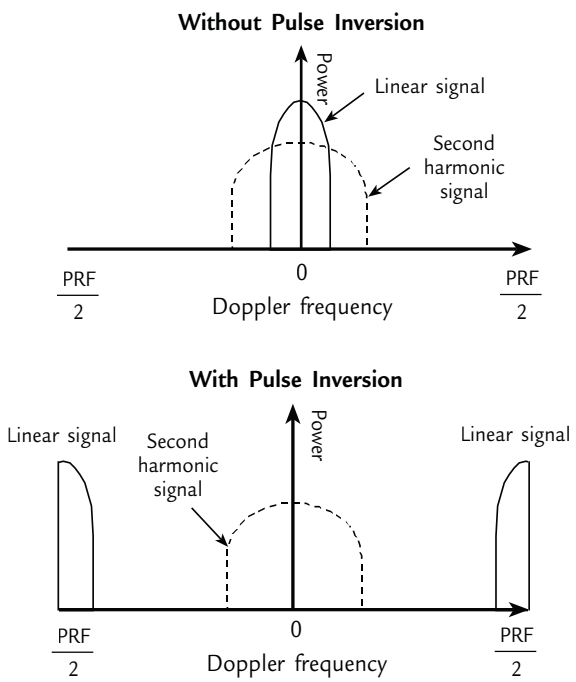

Fig. 6. *Doppler spectra for both linear signal and second harmonic signal. Upper panel: without pulse inversion. Lower panel: with pulse inversion. PRF = pulse repetition frequency.*

spectral overlap between the two signals can be eliminated. As shown in the lower panel, the linear component is shifted to higher frequencies (center at ±PRF/2) with the PI technique. Therefore, separation of the linear signal and the second harmonic signal can be efficiently implemented by filtering.

In human tissues, it is noticeable that the linear component dominates the response. Hence, most of the tissue Doppler signals will be at higher frequencies in the PI Doppler spectra. On the contrary, the blood signal can be highly nonlinear when UCAs are present in the blood pool. In other words, significant second harmonic signals from the blood flow will remain at low Doppler frequencies. Therefore, PI Doppler can be used to distinguish the perfusion region from the surrounding tissue by separating them in the Doppler frequency domain. Clinical success of PI Doppler in perfusion imaging has been reported recently [25]. Although the detection of UCAs is significantly improved by using the PI Doppler technique, the frame rate is reduced since the Doppler estimation must be performed with the responses from multiple transmissions. In addition, the flash artifact associated with color Doppler imaging can also be a problem. Tissue harmonic signals in the background may further limit PI Doppler detection.

RF pulse inversion

In the case of RF pulse inversion, two transmissions are required for each acoustic beam line. After a pulse is transmitted in the first firing, the same pulse is inverted and transmitted again in the second firing. The echoes in both firings are summed together to obtain a beam [26–28]. A schematic diagram of the RF pulse inversion system is shown in Fig. 7. Since the harmonic signal is usually modeled as the power of the fundamental signal $x(t)$, the received echo can be expressed as:

$$y_+(t) = a_1x(t) + a_2x^2(t) + a_3x^3(t) + \cdots \qquad (1)$$

where $a_1x(t)$ represents the linear signal, $a_2x^2(t)$ the second harmonic signal, and $a_3x^3(t)$ the third harmonic signal. Note that the fundamental signal changes from $x(t)$ to $-x(t)$ when the transmit pulse is inverted. Therefore, the echo of the inverted firing will be:

$$y_-(t) = -a_1x(t) + a_2x^2(t) - a_3x^3(t) + \cdots \qquad (2)$$

When the two echoes are summed together, only even-order harmonics remain:

$$\begin{aligned} y_{sum}(t) &= y_+(t) + y_-(t) \\ &= 2a_2x^2(t) + \cdots \end{aligned} \qquad (3)$$

As shown in equation (3), RF pulse inversion can be used to extract the second harmonic signal without interference from any linear signal. In other words, potential spectral leakage in ultrasonic nonlinear imaging may be avoided with the PI technique. In addition, the signal amplitude doubles in the PI sum while the noise level in the sum decreases with a factor of $\sqrt{2}$. Thus, a higher signal-to-noise ratio is expected with the PI technique. Other two-

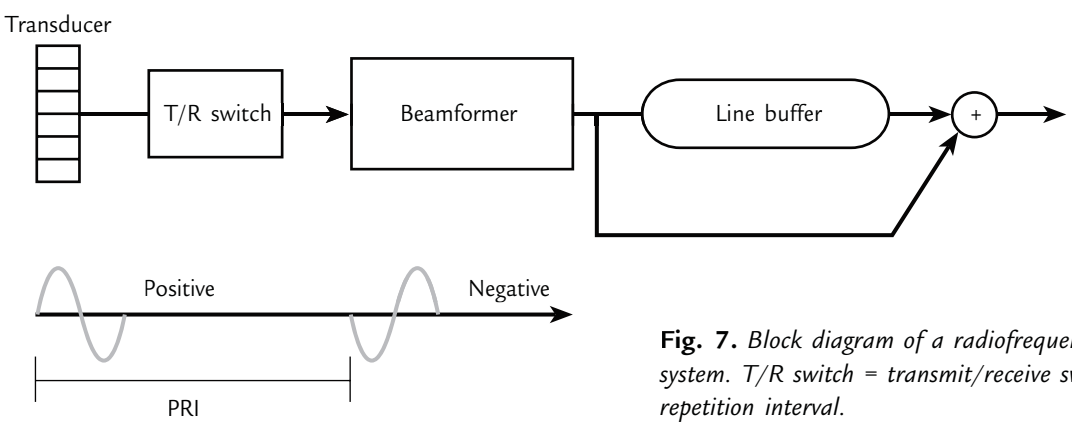

Fig. 7. *Block diagram of a radiofrequency pulse inversion system. T/R switch = transmit/receive switch; PRI = pulse repetition interval.*

pulse approaches use the amplitude modulation (AM) [29] or a combination of AM and PI technique (PIAM) [30]. They achieve a similar cancellation of the linear echoes and preserve some of the odd-order harmonics.

The RF pulse inversion technique can be extended to use more than two pulses. For example, echoes of a phase-coded pulse sequence can be summed to extract the desired harmonic signal [31]. Another approach is based on modeling each of the received echoes as a polynomial of the corresponding transmits. A least squares solution is used to estimate nonlinear components from the received echoes [32]:

$$s_i(t) = \sum_{n=1}^{N} a_n b_i^n q^n(t) \quad i = 1 \ldots I$$

$$\Rightarrow s(t) = \underbrace{\begin{bmatrix} b_1 & b_1^2 & \cdots & b_1^N \\ b_2 & b_2^2 & \cdots & b_2^N \\ \vdots & \vdots & \ddots & \vdots \\ b_I & b_I^2 & \cdots & b_I^N \end{bmatrix}}_{B} \underbrace{\begin{bmatrix} a_1 q \\ a_2 q^2 \\ \vdots \\ a_N q^N \end{bmatrix}}_{x(t)} \qquad (4)$$

$$\Rightarrow x(t) = (B^T B)^{-1} B^T s(t)$$

where the received echo $s_i(t)$ is assumed to be the power combination of the complex transmit pulse b_i and the basis waveform of the nonlinear component $q(t)$. By transmitting I pulses with different phases and magnitudes, the harmonic signal array $x(t)$ can be estimated from the received signal $s(t)$ and the complex pulse matrix B. A similar approach is the contrast pulse sequence, in which echoes from several coded transmissions are combined to extract the third-harmonic signal within the fundamental band [33].

In the following sections, we will focus on the RF pulse inversion technique and its effects on both tissue harmonic imaging and contrast imaging.

Tissue Imaging: Harmonic Leakage Suppression with the PI Technique

In conventional tissue harmonic imaging where the signal is extracted from the received echoes using filtering, spectral leakage of the linear signal to the harmonic band is inevitable, especially when a wideband pulse is used for better axial resolution. Spectral leakage was first considered for contrast harmonic imaging [34]. When the impinging sound wave is near the resonance frequency of the UCAs, the backscattered signal produced by the UCAs at the second harmonic frequency can be several orders of magnitude stronger than the corresponding tissue harmonic signal.

However, image contrast may be reduced in the presence of spectral leakage because the second harmonic signal from surrounding tissue is now increased by these leakage signals. In fact, not only contrast harmonic imaging but also tissue harmonic imaging suffers from potential contrast loss in the presence of spectral leakage [18]. With filtering, the harmonic signal present at a particular imaging depth consists of two components. One is the tissue harmonic signal generated through nonlinear propagation, and the second is the spectral leakage signal produced by the imaging system prior to acoustic propagation. The leakage signals are independent of the nonlinear characteristics of the propagation medium, and produce acoustic beams with different characteristics that may significantly degrade image quality.

The amount of leakage signal significantly depends on the spectral contents of the transmit waveform. For example, the Gaussian pulse has a very band-limited spectrum because of its smooth envelope. Therefore, the leakage signal can be minimized for the Gaussian pulse. Nevertheless, generation of such a transmit waveform is relatively complicated. Typically, a digital waveform buffer and a digital-to-analog converter are required. On the contrary, a gated square wave can be easily synthesized using digital circuits. However, significant harmonic amplitude is present as a result of the sharp transition in the uniform envelope. Fig. 8 shows the Gaussian pulse and the gated square wave in the upper panel. For both waveforms, the center frequency is 2 MHz with a –6 dB 50% fractional bandwidth. The lower panel shows spectra of the convolution of both transmit waveforms

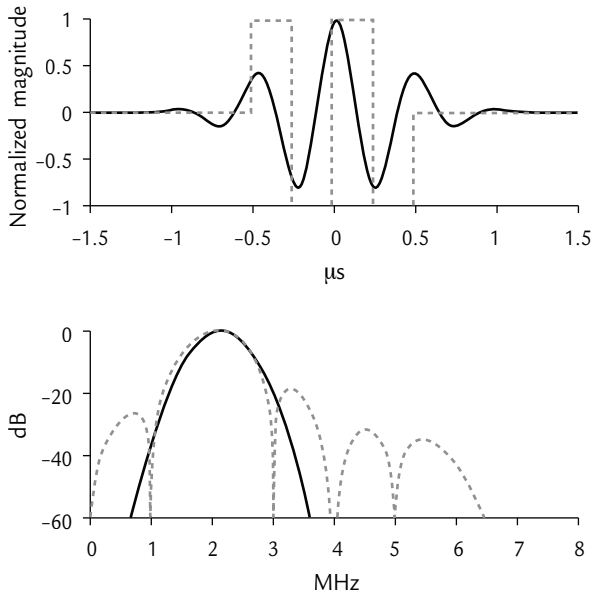

Fig. 8. *Waveforms (upper panel) and spectra (lower panel) of Gaussian pulse (solid line) and gated square wave (dashed line). Center frequency is 2 MHz and fractional bandwidth is 50%.*

with a transducer's frequency response (3 MHz Gaussian with a –6 dB 80% fractional bandwidth). As seen in the spectra, it is clear that the gated square wave may suffer from more severe spectral leakage. In Fig. 9, simulated second harmonic beam patterns of the two transmit waveforms at the transmit focus are shown to illustrate their differences in image contrast. The solid line is for the beam pattern of the Gaussian pulse with 50% bandwidth, and the dashed line is for the gated square wave with 50% bandwidth. Fig. 9 demonstrates clearly that the Gaussian envelope produces significantly lower sidelobes and, thus, produces better image contrast. In addition, for a given type of waveform, the bandwidth also affects the amount of spectral leakage. Waveforms with smaller bandwidths suffer from less spectral leakage and, thus, produce lower sidelobes. This is also shown in Fig. 9 by comparing the solid line (Gaussian pulse with 50% bandwidth) with the dotted line (Gaussian pulse with 25% bandwidth). Although a smaller bandwidth provides lower sidelobes, one drawback is the degraded axial resolution. In other words, a tradeoff exists between axial resolution and image contrast in tissue harmonic imaging with conventional filtering.

Compared to the filtering method, the PI technique can provide better axial and image contrast at the same time. In PI-based tissue harmonic imaging, the echoes from a pair of inverted transmissions are summed to obtain a beam. Since the spectral leakage can be efficiently removed in the PI sum, the transmit waveform with wide bandwidth no longer degrades the contrast resolution in tissue harmonic imaging. In other words, the axial resolution can be improved without sacrificing contrast resolution when a shorter pulse is transmitted. In Fig. 9, a simulated harmonic beam with the PI

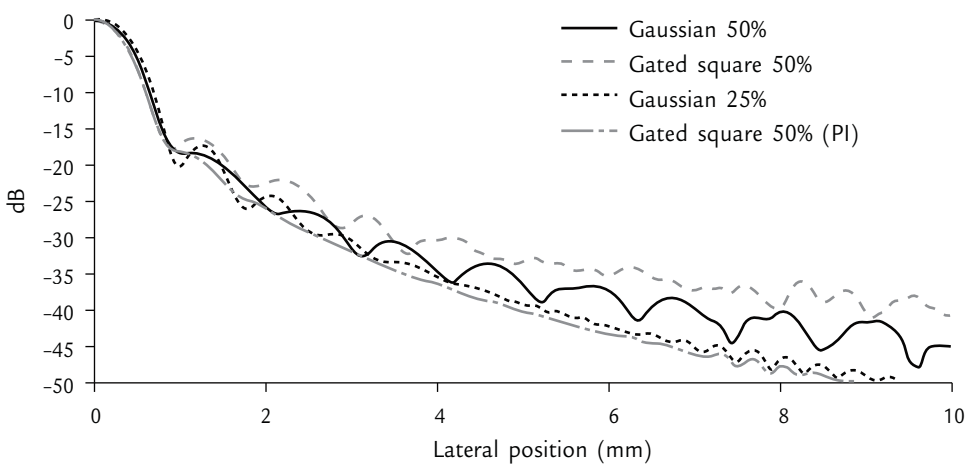

Fig. 9. *Simulated second harmonic beam patterns. The solid line represents the Gaussian pulse with 50% bandwidth (filtering), dashed line the gated square wave with 50% bandwidth (filtering), dotted line the Gaussian pulse with 25% bandwidth (filtering), and dot-dashed line the gated square wave with 50% bandwidth (pulse inversion).*

technique is also depicted. The transmit waveform is the gated square wave with 50% bandwidth. As compared to its counterpart with conventional filtering (dashed line), the beam pattern with the PI technique (dot-dashed line) has much lower sidelobes. Therefore, the PI technique effectively improves image contrast by reducing sidelobe levels. In addition, it is also noticeable that the square wave with the PI technique provides even lower sidelobes than the Gaussian pulses with filtering. Thus, the complexity of the transmit system can be reduced with the PI technique because a simple square waveform is now capable of providing sufficient image contrast.

Contrast Imaging: Improved Contrast Detection with the PI Technique

The PI technique also helps to enhance UCA detection. PI-based methods provide significant improvement in contrast detection by imaging the nonlinearly-generated fundamental signals from microbubbles [30–33,35]. There are several advantages for imaging the nonlinear fundamental signal. First, the passband of the transducer can be fully utilized, enabling the use of broadband transmit pulses for better axial resolution. Second, the transmit and receive passbands can both be around the transducer's center frequency, thereby improving the sensitivity. In addition, unlike in harmonic imaging where the transmit signal is limited to the lower frequency portion of the transducer's passband, the higher transmit center frequencies in PI-based methods result in less microbubble destruction, since the bubble's rupture is more evident at low frequencies [36].

One example of PI-based contrast detection methods is the PI fundamental imaging technique [35]. PI fundamental imaging is based on the observation that the fundamental tissue signal in the PI sum is cancelled out, whereas the fundamental contrast signal is not completely cancelled because the reaction of the bubbles under compression is different from that under rarefaction. In other words, the power model in equation (1), although it works for tissue signals, does not provide an adequate description of the nonlinear bubble response. For example, the positive and negative echoes change from inverted to time-shifted versions of each other as the driving amplitude increases [37]. Besides, a spectral shift was also observed between the center frequencies of the positive echo and the negative echo [38]. When the positive and negative echoes from bubbles are time-shifted and frequency-shifted, uncancelled fundamental signal remains in the PI sum. The PI fundamental signal can be simulated by numerically solving the shell oscillation of a bubble, which can be modeled by the Rayleigh-Plesset equation. The Rayleigh-Plesset equation relates the shell motion with the shell elastic properties and the acoustic pressure [39]. The basic form of the Rayleigh-Plesset equation is:

$$\rho R\ddot{R} + \frac{3}{2}\rho \dot{R}^2 = p_L - p_\infty \qquad (5)$$

where R is the instantaneous bubble radius and ρ is the density of the surrounding liquid. $\dot{R}$ and $\ddot{R}$ are the first and second derivatives of the radius with respect to time, respectively. P_L is the liquid pressure at the shell and P_∞ is the driving pressure. Fig. 10 shows the simulated spectra of a Sonazoid® microbubble. In the simulation, the radius of the bubble is 2 μm, the shear modulus of the shell is

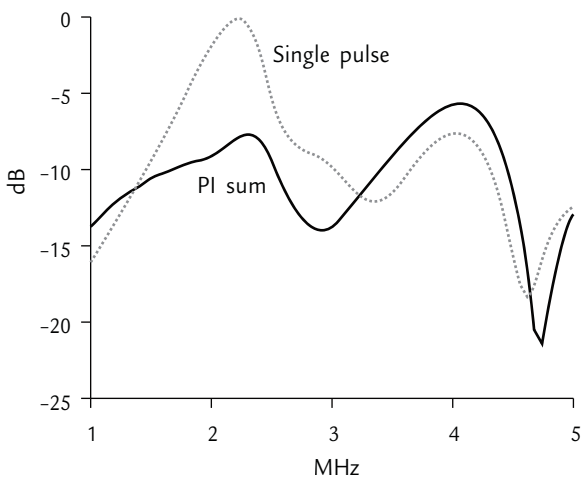

Fig. 10. *Simulated bubble spectra with and without pulse inversion.*

50 MPa, and the shell viscosity is 0.8 Pa·s [37]. The driving waveform is 3 cycles of a gated 2.5-MHz sinusoid with Hanning windowing. The amplitude of the waveform is 300 kPa. Note that in Fig. 10, significant signals remain in both the second harmonic band and the fundamental band even when the PI technique is applied. By imaging the residual fundamental signal in the PI sum, the contrast-to-tissue ratio (CTR) can be enhanced, since the tissue does not generate the PI fundamental signal. Hence, the perfusion region with UCAs can be separated from the background tissue.

Fig. 11 shows the experimental B-mode images of a gelatin-based ultrasonic phantom with Levovist® (Schering AG, Berlin, Germany) microbubbles in a tabular void. The left panel shows the conventional fundamental image, the middle panel is the conventional second harmonic image, and the right panel shows the PI fundamental image. In the left panel, the CTR of the conventional fundamental image is too low to accurately outline the contrast region from the background. Similar difficulty exists in the harmonic image due to the presence of the tissue harmonic signal from the surrounding tissue-mimicking medium. The circular contrast region becomes much more visible in the right panel, demonstrating that the background signal is significantly suppressed in the PI sum and this region is dominated by noise. The CTR values are estimated using mean intensities of the background and the contrast regions indicated by the two boxes in each B-mode image. The CTRs are 17 dB, 19 dB and 37 dB in the left, middle and right panels, respectively, indicating that improvements of 20 dB and 18 dB are obtained over the conventional fundamental and harmonic imaging techniques, respectively, when applying the PI technique in this case. Although the PI fundamental technique is based on the uncancelled fundamental signal, it is still a nonlinear imaging modality since the remaining fundamental signal comes from the nonlinear behavior of the bubbles.

To further enhance contrast detection in PI fundamental imaging, the AM can be included [30]. In the PIAM method, the amplitude of the negative transmission is half of the positive amplitude. The received negative echo is then amplified by a factor of 2 to cancel the linear signal in the PI sum. The PIAM method improves CTR by preserving some of the odd-order harmonics from bubbles in the PI sum. Since the harmonic generation can be modeled as the spectral autoconvolution of a band-limited signal, odd-order harmonics fold back into the transducer's passband and can be effectively detected. In addition, the odd-order harmonics from tissue background can be significantly suppressed by operating the PIAM method in low acoustic power.

Limitations of the PI Technique: Motion Artifacts

Although PI-based imaging methods significantly

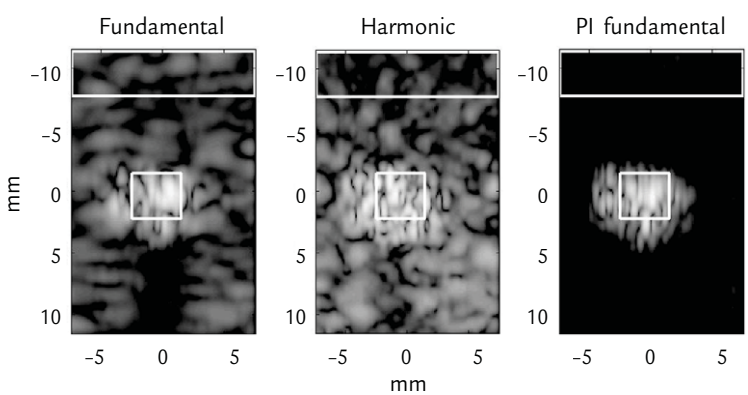

Fig. 11. *B-mode images of a gelatin-based ultrasonic phantom with Levovist® microbubbles in a tabular void [35]. Left panel: conventional fundamental image. Middle panel: conventional harmonic image. Right panel: PI-based fundamental image.*

improve image contrast in ultrasonic nonlinear imaging, their limitations should be considered. Note that two transmissions are required for each beam with the RF pulse inversion technique. Thus, the data acquisition time doubles compared to that with conventional filtering. In other words, temporal resolution (i.e. frame rate) decreases to half. This may pose severe problems in providing dynamic information on fast-moving structures. In addition to the reduced frame rate, motion artifacts may also cause performance loss. In clinical situations, motion artifacts result from the relative movement between the probe and the imaged tissue during the two firings. With motion, the linearly propagating signal is not completely cancelled. In the case of tissue imaging, both the fundamental signal and the spectral leakage remain in the PI sum. Thus, two performance issues should be considered for the motion artifacts in PI-based tissue harmonic imaging. One is the harmonic signal intensity relative to the fundamental intensity, and the other is the potential image quality degradation resulting from spectral leakage [40]. Fig. 12 shows the effects of tissue motion on signal intensities by simulation when only axial motion is considered. The horizontal axis in Fig. 12 is the axial displacement of a point target between two firings normalized to the wavelength at the fundamental frequency (λ). With no displacement, Fig. 12 shows that the PI harmonic signal (dotted line) is at its maximum while the fundamental intensity (solid line) is zero. In clinical applications, tissue motion is most pronounced for cardiac imaging. Based on the typical frequency (1.5–3.5 MHz), myocardial velocity [41] and pulse repetition interval (200–300 μs) used in cardiac imaging, the corresponding displacement could be up to $\lambda/8$. In this range, the PI harmonic signal monotonically decreases and the fundamental signal monotonically increases. Since the fundamental signal is much stronger than the harmonic signal, the fundamental intensity in the PI sum would become larger than the harmonic intensity, even when the displacement is small. As shown in Fig. 12, the fundamental signal becomes dominant in the sum signal when the displacement is only 0.02λ. In other words, filtering is still required to remove the fundamental signal even though the PI technique was originally developed to cancel the linear signal without the need for filtering.

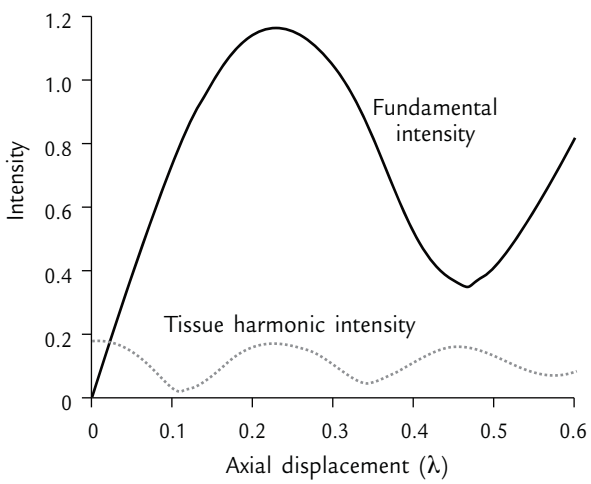

Fig. 12. *Simulated signal intensities as a function of axial motion [40].*

Not only the fundamental signal but also all linear propagating signals increase in the presence of tissue motion, i.e. the spectral leakage signal is also not cancelled in the sum. The leakage signal will interfere with the tissue harmonic signal and degrade image contrast. Fig. 13 shows spectra and tissue harmonic images of an anechoic cyst with a 1.5-MHz transmit frequency. In Fig.13A, spectra of the first scan line are shown and the corresponding B-scan images are illustrated in Fig. 13B. The tissue displacements between the positive pulse and the negative pulse are 0 mm, 0.01 mm and 0.03 mm in the left, middle and right panels, respectively. Spectral leakage is indicated by the elevated fundamental signal level. It is also shown that the anechoic cyst is more contaminated by the leakage harmonic signal when the displacement increases. This agrees well with the increase in spectral leakage.

In comparison with that in tissue harmonic imaging, motion artifacts in PI-based contrast imaging are even more pronounced. PI-based contrast detection takes advantage of the nonlinear fundamental signal from microbubbles to detect UCAs. However, the fundamental signal from the tissue background is strong, so that a small motion may result in a significant uncancelled fundamental sig-

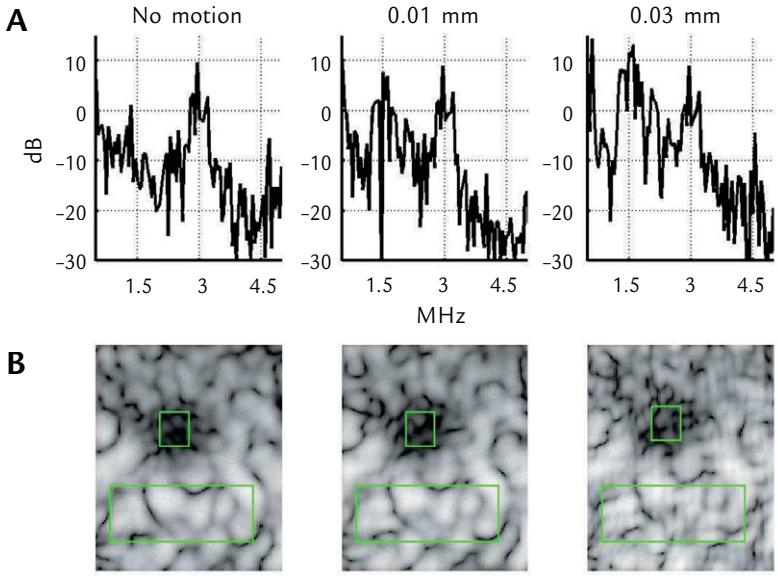

Fig. 13. *Spectra and tissue harmonic images with axial displacements of 0 mm, 0.01 mm and 0.03 mm [40]. The transmit signal was a 1.5-MHz gated sine pulse with a duration of 3 cycles. (A) Spectra. (B) B-scan images.*

nal from the tissue background. In Fig. 14A, PI fundamental images of Levovist® microbubbles associated with different axial motions are shown. The displacements between the positive and negative pulses were 0.015 mm and 0.03 mm, corresponding to velocities of 5 cm/s and 10 cm/s for the pulse repetition interval of 300 μs. It can be seen in the figure that the background intensity increases with tissue motion. The CTR improvement as a function of tissue displacement is plotted in Fig. 14B, which demonstrates that the CTR is highly sensitive to tissue motion (decreasing by 17 dB from no motion to a 0.015-mm displacement). Hence, motion compensation is essential for PI-based contrast detection when the fundamental signal is used for imaging.

Motion artifacts are even more severe when more firings are used to extract harmonic signals for each beam line. For example, the phase-coded pulse sequence with three pulses can be used to extract the third harmonic signal. In this case, phases of the pulses are 0°, 120° and 240°, respectively [31]. Because the time needed for each sum signal increases, the multiple-firing scheme is more susceptible to motion. A simple scheme may be employed to correct for the motion artifacts. A correlation-based time shift estimator may be adopted to estimate and compensate for the phase difference

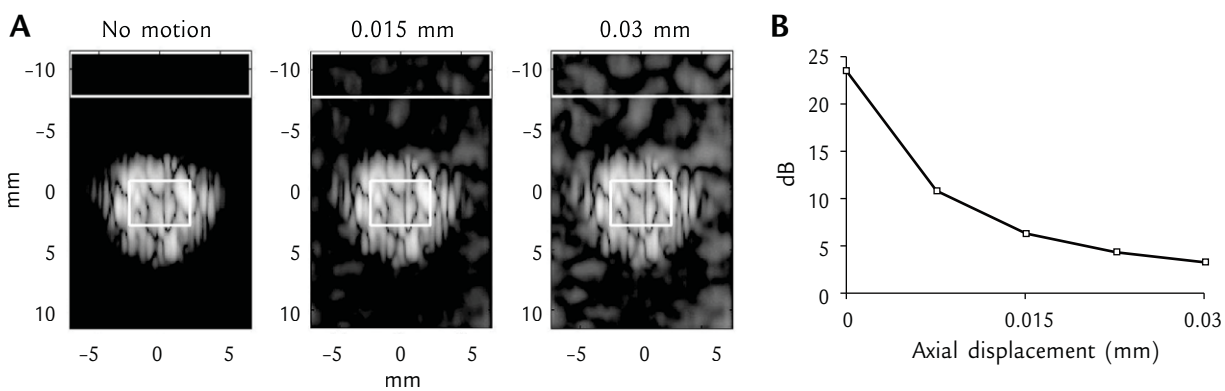

Fig. 14. *(A) PI fundamental images for axial displacements of 0 mm, 0.015 mm and 0.03 mm [35]. (B) Contrast-to-tissue ratio improvement as a function of axial displacement.*

introduced by the motion between the positive echo and the negative echo [42]. Nevertheless, it has been shown that the correction scheme effectively removes motion artifacts only when the axial motion is considered, and little improvement is obtained with lateral motion correction [40]. This is because the simple correlation-based method only accounts for axial motion. Since the 1-dimensional correlation-based method generally does not estimate lateral motion, 2-dimensional motion correction is required.

Note that the PI Doppler technique does not directly suffer from the aforementioned intensity variation and contrast degradation. This is due to the fact that the positive echo and the negative echo are not summed together to obtain the harmonic signal. Instead, a clutter filter is applied to the Doppler signal.

Concluding Remarks

In ultrasonic nonlinear imaging, the PI technique plays an effective role in improving image quality. By applying the PI technique to either the Doppler domain or the RF domain, interference from the linear signal can be avoided and, thus, more diagnostic information can be provided. PI Doppler takes advantage of interleaved positive and negative firings in the Doppler estimation to separate the nonlinear Doppler signal from the linear Doppler signal. On the other hand, echoes from a pair of inverted transmits are summed to cancel the linear signal in the RF pulse inversion technique. In this review paper, the efficacy and limitations of the PI technique have been discussed in detail.

In tissue harmonic imaging, image contrast is degraded when significant spectral leakage is present in the harmonic band prior to the nonlinear generation of the tissue harmonic signal. Compared to conventional filtering, the tradeoff between image contrast and axial resolution is eliminated by canceling the spectral leakage in the PI sum. Furthermore, the signal-to-noise ratio is also improved because the tissue harmonic signals in both firings are summed coherently, resulting in enhanced signal intensity.

In contrast imaging, the PI technique helps to detect UCAs on the basis of the nonlinear characteristics of the microbubbles. In the case of PI Doppler detection, the contrast agents can be successfully distinguished from the linear background in the Doppler frequency domain. Nevertheless, flash artifacts and frame rate reduction can be problematic. In addition, tissue harmonic signals in the background may further limit PI Doppler detection. The B-mode PI-based contrast imaging methods are also illustrated. For example, the CTR in PI fundamental imaging is improved based on the observation that the fundamental signal in the PI sum is not completely cancelled for UCAs. By imaging the fundamental residual signal in the PI sum, a higher CTR is obtained in comparison with that in conventional fundamental imaging or second harmonic imaging.

When the imaged tissue moves during the PI firings, potential motion artifacts should be considered. It is shown that the tissue harmonic signal is highly susceptible to tissue motion, and the linear signal increases with motion. Motion artifacts also degrade the image contrast in tissue harmonic imaging because the leakage signal is not cancelled in the PI sum due to motion. Compared to that in tissue harmonic imaging, motion artifacts become even more pronounced in PI-based contrast imaging because the tissue fundamental signal in the background is much stronger. Thus, motion estimation and compensation should be included in PI-based imaging.

PI-related studies are still active. PI technique in high frequency applications for detecting submicron bubbles has recently been reported [43]. In this case, separation of the bubbles from the surrounding tissue is improved since the significant spectral overlap between the transmit signal and the subharmonic echoes from the microbubbles is suppressed in the PI sum. It has also been reported that coded transmit has potential to further improve contrast detection in PI fundamental imaging [44, 45].

References

1. Gramiak R, Shah PM, Kramer DH. Ultrasound cardiography contrast studies in anatomy and function. *Radiology* 1969;92:939–48.
2. Ophir J, Parker KJ. Contrast agents in diagnostic ultrasound. *Ultrasound Med Biol* 1989;15:319–33.
3. Simpson DH, Burns PN. Perfusion imaging with pulse inversion Doppler and microbubble contrast agents: *in vivo* studies of the myocardium. *IEEE Ultrason Symp Proc* 1998:1783–6.
4. Tranquart F, Grenier N, Pourcelot VEL. Clinical use of ultrasound tissue harmonic imaging. *Ultrasound Med Biol* 1999;25:889–94.
5. Desser TS, Jeffrey RB. Tissue harmonic imaging techniques: physical principles and clinical applications. *Semin Ultrasound CT MR* 2001;22:1–10.
6. Beyer RT, Letcher SV. *Nonlinear Acoustics.* New York: Academic Press, 1969:202–30.
7. Haran ME, Cook BD. Distortion of finite amplitude ultrasound in lossy media. *J Acoust Soc Am* 1983;73: 774–9.
8. Cain CA. Ultrasonic reflection mode imaging of the nonlinear parameter B/A: I. A theoretical basis. *J Acoust Soc Am* 1986;80:28–32.
9. Hamilton MF, Blackstock DT. *Nonlinear Acoustics.* San Diego, CA: Academic Press, 1998.
10. Duck FA. Nonlinear acoustics in diagnostic ultrasound. *Ultrasound Med Biol* 2002;28:1–18.
11. Goldberg BB, Liu JB, Forsberg F. Ultrasound contrast agents: a review. *Ultrasound Med Biol* 1994;20:319–33.
12. Goldberg BB. *Ultrasound Contrast Agents.* London: M. Dunitz, 1997.
13. Chang PH, Shung KK, Wu SJ, et al. Second harmonic imaging and harmonic Doppler measurements with Albunex®. *IEEE Ultrason Ferroelec Freq Control* 1995;42: 1020–7.
14. de Jong N. Improvements in ultrasound contrast agents. *IEEE Eng Med Biol* 1996;15:72–82.
15. Shi WT, Forsberg F. Ultrasonic characterization of the nonlinear properties of contrast microbubbles. *Ultrasound Med Biol* 2000;26:93–104.
16. Dayton PA, Morgan KE, Klibanov AL, et al. Optical and acoustical observations of the effects of ultrasound on contrast agents. *IEEE Ultrason Ferroelec Freq Control* 1999;46:220–32.
17. Dayton PA, Morgan KE, Klibanov AL, et al. A preliminary evaluation of the effects of primary and secondary radiation forces on acoustic contrast agents. *IEEE Ultrason Ferroelec Freq Control* 1997;44:1264–77.
18. Shen CC, Li PC. Harmonic leakage and image quality degradation in tissue harmonic imaging. *IEEE Ultrason Ferroelec Freq Control* 2001;48:728–36.
19. Li PC, Shen CC. Effects of transmit focusing on finite amplitude distortion based second harmonic generation. *Ultrason Imaging* 1999;21:243–58.
20. Averkiou MA, Roundhill DN, Powers JE. A new imaging technique based on the nonlinear properties of tissues. *IEEE Ultrason Symp Proc* 1997:1561–6.
21. Christopher T. Finite amplitude distortion-based inhomogeneous pulse echo ultrasonic imaging. *IEEE Ultrason Ferroelec Freq Control* 1997;44:125–39.
22. Ward B, Baker AC, Humphrey VF. Nonlinear propagation applied to the improvement of resolution in diagnostic medical ultrasound equipment. *J Acoust Soc Am* 1997;10:143–54.
23. Simpson DH, Burns PN. Pulse inversion Doppler: a new method for detecting nonlinear echoes from microbubble contrast agents. *IEEE Ultrason Symp Proc* 1997:1597–600.
24. Simpson DH, Chin CT, Burns PN. Pulse inversion Doppler: a new method for detecting nonlinear echoes from microbubble contrast agents. *IEEE Ultrason Ferroelec Freq Control* 1999;46:372–82.
25. Bruce M, Averkiou M, Tiemann K, et al. Vascular flow and perfusion imaging with ultrasound contrast agents. *Ultrasound Med Biol* 2004;30:735–43.
26. Chapman CS, Lazenby JC. Ultrasound imaging system employing phase inversion subtraction to enhance the image. *US Patent No. 5,632,277*, 1997.
27. Wright NJ, Maslak SH, Finger DJ, et al. A method and apparatus for coherent image formation. *US Patent No. 5,667,373*, 1997.
28. Jiang P, Mao Z, Lazenby JC. A new harmonic imaging scheme with better fundamental frequency cancellation and higher signal-to-noise ratio. *IEEE Ultrason Symp Proc* 1998:1589–94.
29. Brock-Fisher G, Poland M, Rafter P. Means for increasing sensitivity in nonlinear ultrasound imaging systems. *US Patent No. 5,577,505*, 1996.
30. Eckersley RJ, Chin CT, Burns PN. Optimising phase and amplitude modulation schemes for imaging microbubble contrast agents at low acoustic power. *Ultrasound Med Biol* 2005;31:213–9.
31. Wilkening W, Krueger M, Ermert H. Phase-coded pulse sequence for non-linear imaging. *IEEE Ultrason Symp Proc* 2000:1597–600.
32. Haider B, Chiao RY. Higher order nonlinear ultrasonic imaging. *IEEE Ultrason Symp Proc* 1999:1527–31.
33. Phillips PJ. Contrast pulse sequences (CPS): imaging nonlinear microbubbles. *IEEE Ultrason Symp Proc* 2001:

1739–45.
34. Krishnan S, O'Donnell M. Transmit aperture processing for non-linear contrast agent imaging. *Ultrason Imaging* 1996;18:77–105.
35. Shen CC, Li PC. Pulse-inversion-based fundamental imaging for contrast detection. *IEEE Ultrason Ferroelec Freq Control* 2003;50:1124–33.
36. Uhlendorf V, Hoffman C. Nonlinear acoustical response of coated microbubbles in diagnostic ultrasound. *IEEE Ultrason Symp Proc* 1994:1559–62.
37. Hoff L. Nonlinear response of sonazoid. Numerical simulation about pulse-inversion and subharmonics. *IEEE Ultrason Symp Proc* 2000:1885–8.
38. Morgan KE, Averkiou M, Ferrara KW. The effect of the phase of transmission on contrast agent echoes. *IEEE Ultrason Ferroelec Freq Control* 1998;45:872–5.
39. Frinking PJA, de Jong N. Acoustic modeling of shell-encapsulated gas bubbles. *Ultrasound Med Biol* 1998;24: 523–33.
40. Shen CC, Li PC. Motion artifacts of pulse inversion based tissue harmonic imaging. *IEEE Ultrason Ferroelec Freq Control* 2002;49:1203–11.
41. Shan K, Bick RJ, Poindexter BJ, et al. Relation of tissue Doppler derived myocardial velocities to myocardial structure and beta-adrenergic receptor density in humans. *J Am Coll Cardiol* 2000;36:891–6.
42. Nock LF, Trahey GE. Synthetic receive aperture imaging with phase correction for motion and for tissue inhomogeneities—Part I: basic principles. *IEEE Ultrason Ferroelec Freq Control* 1992;39:489–95.
43. Goertz DE, Frijlink ME, de Jong N, et al. High frequency nonlinear scattering and imaging of a submicron contrast agent. *IEEE Ultrason Symp Proc* 2004:986–9.
44. Cheng YC, Li PC. The applications of coded waveform in pulse inversion fundamental imaging. *Annual Symposium of the Biomedical Engineering Society*, Chung-Li, Taiwan, 2005.
45. Shen CC. *Pulse Inversion Based Ultrasonic Nonlinear Imaging.* Taipei, Taiwan: National Taiwan University, 2005. [Dissertation]